Available online at www.sciencedirect.com
SCIENCE DIRECT®

Journal of the European Ceramic Society 24 (2004) 2583–2589
www.elsevier.com/locate/jeurceramsoc

Microwave dielectric properties of $(1-x)CeO_2$–$xCaTiO_3$ and $(1-x)CeO_2$–xSm_2O_3 ceramics

M.T. Sebastian[a,b], N. Santha[a,b], P.V. Bijumon[a], Anna-Karin Axelsson[b,*], Neil McN. Alford[b]

[a]*Ceramics Division, Regional Research Laboratory, Trivandrum 695019, India*
[b]*Physical Electronics and Materials, South Bank University, London SE1 OAA, UK*

Received 18 May 2003; accepted 27 September 2003

Abstract

CeO_2–$CaTiO_3$ and CeO_2–Sm_2O_3 microwave dielectric ceramics have been prepared by a conventional solid state ceramic route. The dielectric ceramics are characterized by X-ray diffraction, SEM, Raman and microwave methods. Ceria has a relative dielectric constant, ε_r, of 23, high dielectric quality factor×frequency product, $Q\times f$ up to 60,000 GHz with high temperature coefficient of resonant frequency, τ_f, of −53 ppm/°C. The addition of $CaTiO_3$ and samarium oxide leads to a zero temperature variation of resonant frequency. The relative dielectric constant increases and Q decrease with $CaTiO_3$ addition and the τ_r changes from a negative to a positive value. Sm_2O_3 addition of up to 50 mol% increases Q, decreases ε_r and improves the τ_f. The microwave dielectric properties are measured at low temperatures down to 20 K. The effect of addition of 1 mol% of various rare earth oxides on the microwave dielectric properties of ceria has also been investigated.

Keywords: CeO_2; Sm_2O_3; $CaTiO_3$; Microwave ceramics; Dielectric resonators

1. Introduction

Several research groups have developed microwave dielectric resonators (DRs) with satisfactory dielectric properties.[1] Ceramic materials for DR applications should have high quality factor (Q), high relative permittivity (ε_r) and the stability of these parameters in the working temperature and frequency ranges. Ceria-based materials have been intensively investigated as catalysts, structural and electronic promoters of heterogeneous catalytic reactions and oxide ion conducting solid electrolytes in electrochemical cells.[2] Recently we showed ceria to be a good dielectric resonator material with a $\varepsilon_r = 23$, quality factor ($Q\times f$) of about 60,000. We also demonstrated that the addition of 1 mol% $CaCO_3$ increases the Q.[3] But the temperature coefficient of resonant frequency (τ_f) of ceria has a large negative value (−53 ppm/°C), which precludes its use in practical applications. It is possible to achieve temperature compensation by preparing a solid solution phase between compounds having positive and negative τ_f values.[4–8] The perovskite $CaTiO_3$ has[9] a high positive value of τ_f (800 ppm/°C). In the present work we report the microwave dielectric properties of ceria with different amounts of additives such as $CaTiO_3$ and Sm_2O_3 which exhibit a positive values of τ_f'. The effect of various rare earth oxides on the microwave dielectric properties of ceria has also been investigated.

2. Experimental

The dielectric samples were prepared by a conventional solid-state ceramic route. CeO_2, Sm_2O_3, $CaCO_3$, and TiO_2 with purity >99.9% were used as starting materials. Cerium oxide and Sm_2O_3 were calcined at 800 °C for 3 h to remove volatile impurities. The powders were weighed according to the compositions $(1-x)CeO_2$–xSm_2O_3 ($x = 0.005$, 0.01, 0.10, 0.30, 0.50, 0.70, 0.80, 0.90 and 0.95) and $(1-x)CeO_2$–$xCaTiO_3$($x = 0.01$, 0.02, 0.04, 0.06, 0.08, 0.10) and mixed in an agate mortar using distilled water and then dried.

* Corresponding author.
E-mail addresses: mailadils@yahoo.com (M.T. Sebastian), alfordn@lsbu.ac.uk (A.-K. Axelsson).

0955-2219/$ - see front matter © 2003 Elsevier Ltd. All rights reserved.
doi:10.1016/S0955-2219(03)00782-9

The mixed powder was calcined at 1200 °C for 4 h. In the CeO_2–Sm_2O_3 system, the samples with higher contents of Sm_2O_3 decomposed or become fine powder on aging. To avoid this, 0.5 wt.% CuO was added to the calcined powder for $x=0.90$ and 0.95. A 5% PVA solution was added to the powder as a binder and the slurry was dried. The resulting powders were again ground well and then uniaxially pressed into pellets 14 mm in diameter and about 7 mm in height. These pellets were sintered at 1600–1650 °C for 4 h. The preferred sintering temperatures were chosen to be the temperature resulting in the highest sample density. Samples of ceria with 1 mol% of dopant (Nd_2O_3, Sm_2O_3, Eu_2O_3, Gd_2O_3 and Er_2O_3) were also prepared as described above.

Powder X-ray diffraction (XRD) patterns of $(1-x)$ CeO_2–xSm_2O_3 and $(1-x)CeO_2$–$xCaTiO_3$ were taken using CuK_α radiation as a function of composition to investigate the crystalline structure. The density of the ceramic pucks was determined by the Archimedes method. Scanning electron micrographs were recorded from thermally etched samples using Hitachi SEM model No. S-4300.

Dielectric properties at microwave frequencies were measured in the 4–6 GHz frequency range. The end-shorted method proposed by Hakki and Coleman[10] and later modified by Courtney[11] was employed for the evaluation of the relative dielectric constant using the TE_{011} mode. The dielectric quality factor of the samples was measured by the cavity method[12] using the $TE_{01\delta}$ resonant mode. The temperature coefficient of resonant frequency was measured by noting the response of the TE_{011} mode with respect to temperature using the Hakki and Coleman method in the 20–80 °C region. The low temperature microwave dielectric properties were measured by placing the cavity on the cold head of a closed cycle Gifford McMahon ciyostat (“workhorse”, Cryophysics, Abingdon, UK) and the microwave dielectric properties were determined using a vector network analyzer (HP8720C) in the temperature range 20–300 K. The Raman spectra from the sintered pucks were recorded using a Renishaw system 2000 microprobe with a 488 nm line of an Ar+ laser as exciting radiation with nominally <4.0 mW power incident on the sample surface. The laser line was focused onto the sample by a cylindrical microscope lens of ×50 magnification with a spot diameter of 3 ± 1 μm.

3. Results and discussion

3.1. $(1-x)$ CeO_2–$xCaTiO_3$ $(0.1\leqslant x\leqslant 0)$ ceramics

Pure CeO_2 has a cubic fluorite type of structure with space group Fm3m and has a density of 7.215 g cm^{-3} (JCPDS file no. 43-1002). It has $\varepsilon_r=23$, $Q\times f>60{,}000$ (at 6 GHz) and $\tau_f=-53$ ppm/°C.[3]

Fig. 1 shows the X-ray diffraction patterns recorded from $(1-x)$ CeO_2–$xCaTiO_3$ indicating the single phase nature of the ceramics. Fig. 2a shows the scanning electron micrograph recorded from pure CeO_2 and Fig. 2b $0.9CeO_2$–$0.1CaTiO_3$ ceramic. Pure ceria grains are large in size 20–25 μm where as the $0.9CeO_2$–$0.1CaTiO_3$ ceramic the grains are about 10 μm in size although both sintered at the same temperature. The SEM picture also shows the single phase nature of the ceramics.

The Raman spectra of $CaTiO_3$-doped CeO_2 were measured for composites $x<0.06$ and given in Fig. 3. Pure CeO_2 has a Raman active mode (F_{2g}) at 465 cm^{-1} which is attributed to the symmetrical stretching mode of the Ce-O8 vibration making this mode suitable for detecting oxygen disorder. An increased addition of $CaTiO_3$ caused only a minor shift of the 465 cm^{-1} mode from 465.6 to 465.3 cm^{-1} and an increase in the linewidth (FWHM) from 10.6 to 12.1 cm^{-1}. The formed single phase is proceeded by substitution of Ce^{4+} in the lattice by Ti^{4+} and Ca^{2+} where it has been suggested in earlier FTIR study[3] that Ti addition decreases anharmonicity in the lattice by decreasing multiphonon absorption and Ca increases anharmonicity.

The sintered densities of the specimens, relative to the $CaTiO_3$ content are plotted in Fig. 4. The density increases with a small addition of $CaTiO_3$ ($x=0.02$), but with further addition of $CaTiO_3$, it decreases.

Fig. 5 shows the relationship between the ε_r and the composition (x) compared with those obtained by the logarithmic mixing rule $\ln\varepsilon_r=V_1\ln\varepsilon_{r1}+V_2\ln\varepsilon_{r2}$ where V_1 and V_2 are volume fractions of each component, ε_{r1} and ε_{r2} are their relative dielectric constant and ε_r is the

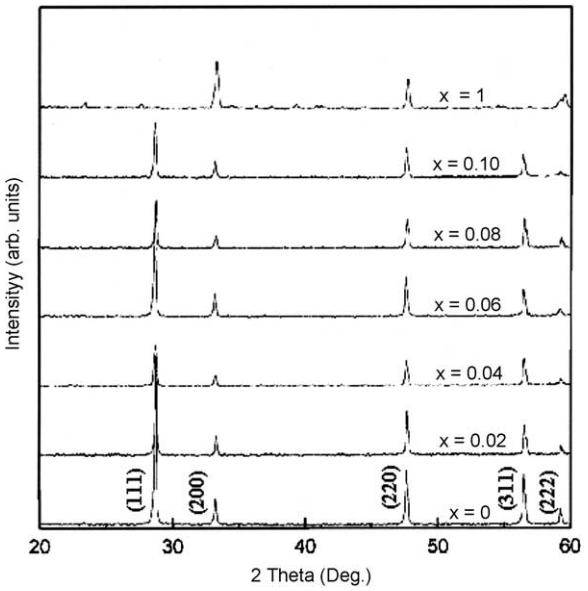

Fig. 1. Powder X-ray diffraction patterns of $(1-x)CeO_2$–$xCaTiO_3$ ceramics.

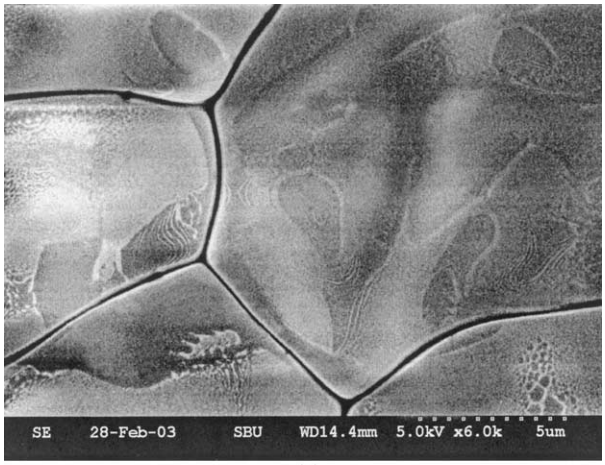

Fig. 2. Scanning electron micrographs recorded from thermally etched samples: (a) CeO_2×6000; (b) $0.9CeO_2$–$0.1CaTiO_3$×3000.

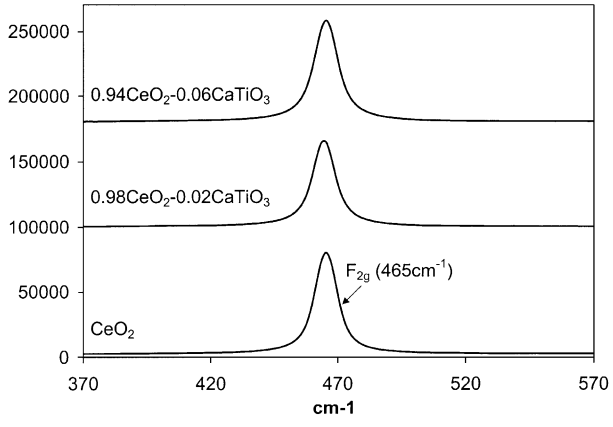

Fig. 3. Raman spectra of $(1-x)CeO_2$–$xCaTiO_3$ ceramics for different values of x.

resultant relative dielectric constant of the mixture.[13] The ε_r increases with the increasing $CaTiO_3$ content. This is expected since $CaTiO_3$ has a high ε_r of 170.[9] Fig. 5 shows that the measured ε_r is slightly higher than those calculated by the mixture rule. Fig. 4 shows the

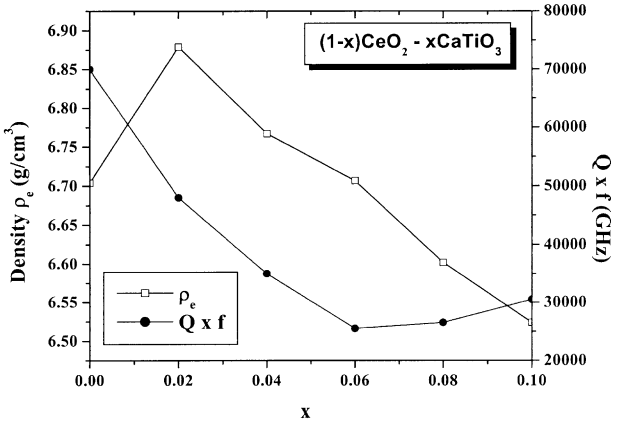

Fig. 4. The variation of experimental density and $Q\times f$ of $(1-x)CeO_2$–$xCaTiO_3$ ceramics as a function of $CaTiO_3$ content.

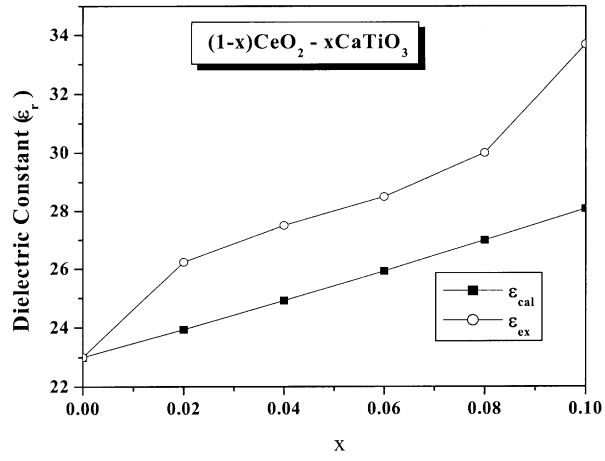

Fig. 5. Variation of experimental and calculated ε_r using the mixture rule with composition in the $(1-x)CeO_2$–$xCaTiO_3$ system.

effect of $CaTiO_3$ addition on the quality factor ($Q\times f$). The quality factor decreases with $CaTiO_3$ addition. Fig. 6 shows the quality factor ($Q\times f$) of CeO_2–$CaTiO_3$ measured at low temperatures in the range 20–300 K. The increase in the quality factor is rather small on cooling until 130 K. Further cooling increases the Q considerably but much less when compared with pure ceria.

Fig. 7 shows the variation of τ_f with composition in $(1-x)$ $CaTiO_3$–$xCeO_2$ $(0.9\leqslant x\leqslant 1)$ ceramics. The τ_f varies from −53 to +60 ppm/°C as x varies from 0 to 0.1. The temperature compensation (zero τ_f) occurs at $x=0.057$.

3.2. $(1-x)$ CeO_2–xSm_2O_3 ceramics

Sm_2O_3 has two phases; monoclinic with density 7.746 g cm^3 [JCPDS File No. 42-1464] and cubic with density 7.103 g cm^3 [JCPDS File No.15-813]. The XRD pattern recorded from crushed powders from sintered compacts of $(1-x)$ CeO_2–xSm_2O_3 $(0\leqslant x\leqslant 1)$ ceramics are shown

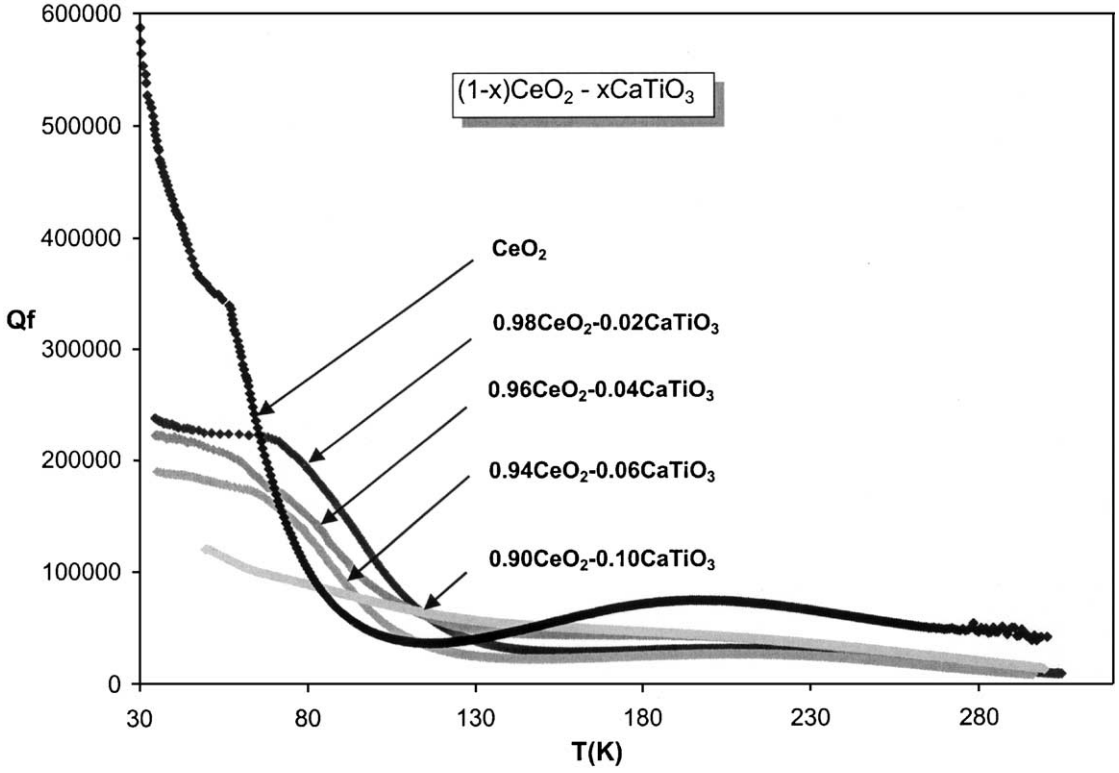

Fig. 6. Variation of quality factor ($Q\times f$ GHz) of $(1-x)CeO_2$–$xCaTiO_3$ ceramics as a function of temperature.

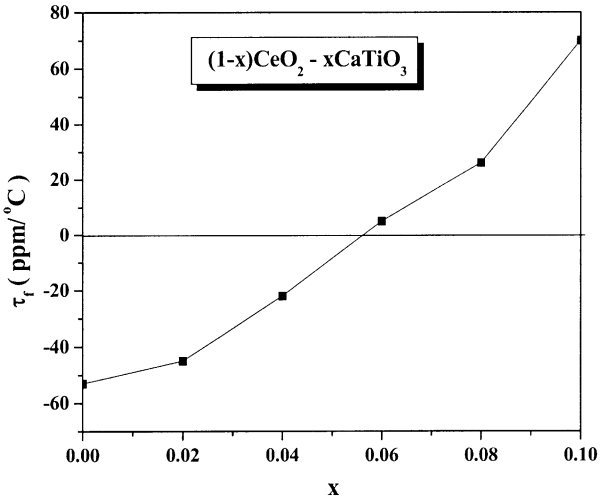

Fig. 7. Temperature coefficient of resonant frequency (τ_f) of $(1-x)CeO_2$–$xCaTiO_3$ ceramics as a function of composition x.

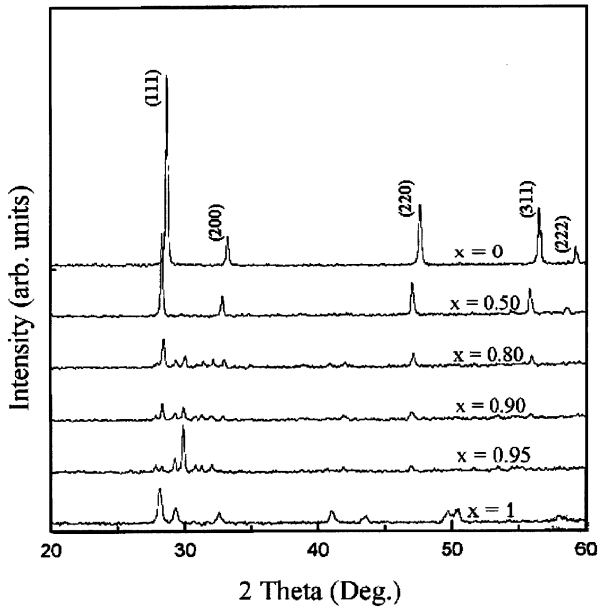

Fig. 8. The powder X-ray diffraction patterns of $(1-x)CeO_2$–xSm_2O_3 ceramics.

in Fig. 8. The compositions with $x=0$–0.5 showed a cubic fluorite structure as evidenced by the XRD in Fig. 8 which is in agreement with Peng et al.[14] The CeO_2–Sm_2O_3 sintered into dense ceramic. Fig. 9 shows the variation of density with composition. The density initially decreases and then increases with increase in Sm_2O_3 content. Fig. 10 show the SEM images from $0.5CeO_2$–$0.5Sm_2O_3$ ceramic, indicating a single phase nature. The SEM photographs show dense ceramic with grain size up to 10 μm that are smaller in size as compared to pure ceria. The XRD patterns recorded from samples with $x>0.5$ are in agreement with the monoclinic symmetry Sm_2O_3. The Sm_2O_3 sintered up to 99% of the theoretical density (7.746 g cm^3). The sintered Sm_2O_3 has $\varepsilon_r=23$, $\tau_f=+22$ ppm/°C and $Q\times f=46{,}000$ GHz. However the sintered samples decomposed and

became powder on aging. Addition of 0.5 wt.% of CuO prevented the decomposition problem.

Fig. 11 shows the Raman spectra of Sm-doped CeO_2 for compositions were $X<0.5$. The linewidth (FWHM) of the 465 cm^{-1} mode increases up to $X=0.2$ (from 10.5 to 37.3 cm^{-1}) and thereafter decreases to 27.3 cm^{-1} at $X=0.5$. The same mode, which can be viewed as an indication of the Ce-O8 vibrations, shifts first to lower frequency when X goes to 0.1 (from 465.5 to 463.5 cm^{-1}) before shifting higher to 473.1 cm^{-1} at $X=0.3$ and finally lower again to 469.5 cm^{-1} at $X=0.5$. These shifts are due to the change of oxygen vacancies and valency changes which are introduced into the CeO_2 lattice when Sm^{3+} substitute the Ce^{4+}. Additional modes appears with more samarium addition where most noticeable are a couple of soft modes at 554 and 589 cm^{-1}. The theory of changes of oxygen vacancies, which in return causes intrinsic losses, are supported by comparing the dielectric loss at low temperatures where a small addition of Sm ($X=0.01$) decreases the loss of pure CeO_2 at 100 K and by further addition of Sm, up to $X=0.5$, a steady decrease of the loss appear at the same temperature.

The maximum solubility of samarium into the lattice is about $X=0.5$.[14] This can be observed in a drastic change of both ε_r and Q at $X=0.5$ as shown in Fig. 12. The similar ionic size between Ce^{4+} and Sm^{3+} contribute to a much higher solubility than the $CaTiO_3$ doped composites. The variation of ε_r and $Q\times f$ of the $(1-x)CeO_2$–xSm_2O_3 as a function of x are shown in Fig. 12. The ε_r of both Sm_2O_3 and CeO_2 are nearly the same and so it is expected that ε_r of the system remains almost the same through out the region under study. However there is a decrease in the ε_r in the region $0.01\leqslant x\leqslant 0.50$, which can be attributed to the decrease in relative density. The $Q\times f$ increases from 70,000 to 90,000 GHz as x varies from zero to 0.5 and further increase in x decreases the quality factor. The τ_f increases from −53 ppm/°C with increase in x and becomes positive value as shown in Fig. 13. The τ_f becomes zero for $x=0.92$.

Fig. 14 shows the variation of the quality factor on cooling the ceramic samples down to 20 K. In the case of CeO_2 the quality factor increases rapidly on cooling. The percentage increase in the quality factor on cooling

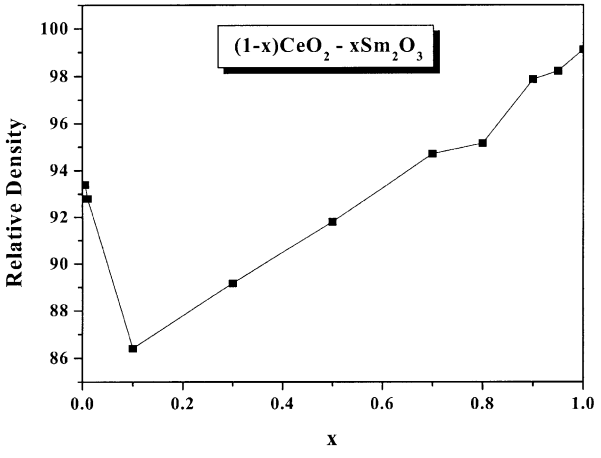

Fig. 9. Variation of the relative density of $(1-x)CeO_2$–xSm_2O_3 ceramics as a function of composition x.

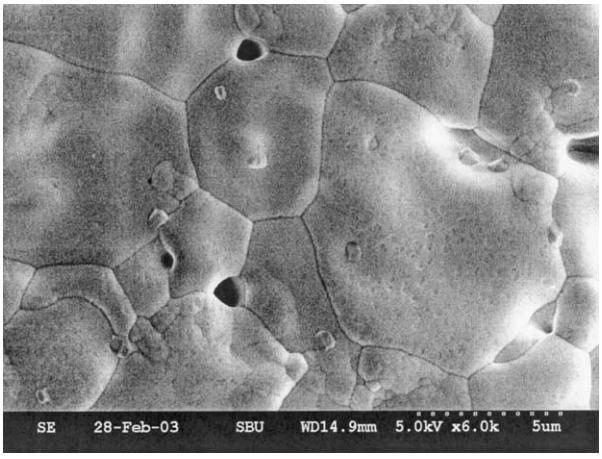

Fig. 10. Scanning electron micrograph of $0.5CeO_2$–$0.5Sm_2O_3$ ceramic.

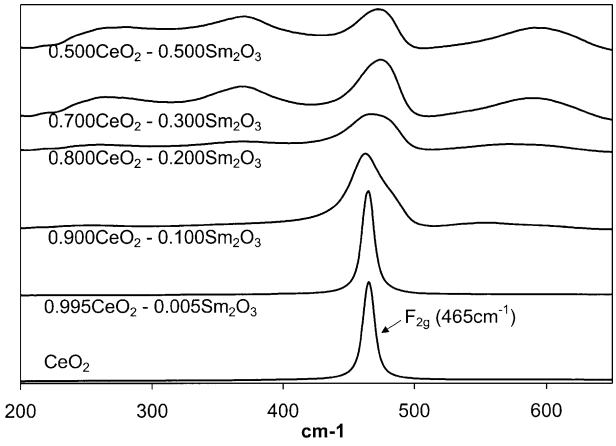

Fig. 11. Raman spectra of $(1-x)CeO_2$–xSm_2O_3 ceramics for different values of x.

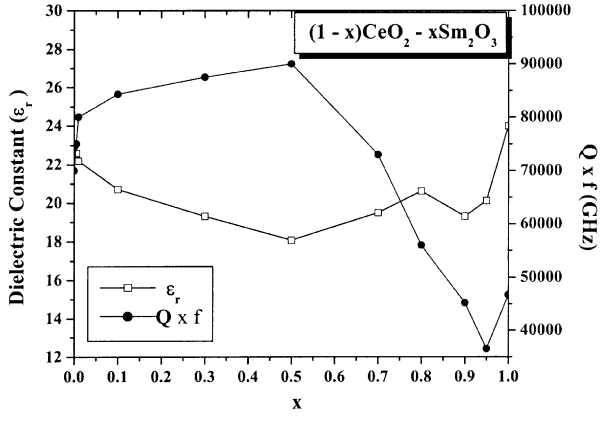

Fig. 12. Variation of ε_r and $Q\times f$ GHz of $(1-x)CeO_2$–xSm_2O_3 ceramics as a function of composition x.

decreases with increase in Sm_2O_3 content. For 50 mol% Sm_2O_3 addition, there is hardly any increase in the Q value on cooling. The $0.5CeO_2$–$0.5Sm_2O_3$ has the highest Q at room temperature. The quality factor–temperature plot shows a dip or lowering of Q at about 100 K.

In order to study the effect of various rare earth ions with different ionic radii on the microwave dielectric properties of ceria 1 mol% each of rare oxide such as Nd_2O_3, Eu_2O_3, Gd_2O_3 and Er_2O_3 was added to calcined CeO_2 and pellets were prepared. The microwave dielectric properties of these rare earth doped ceria are tabulated in Table 1. Table 1 shows that microwave dielectric properties of ceria does not depend on the radii of the rare earth dopant ion.

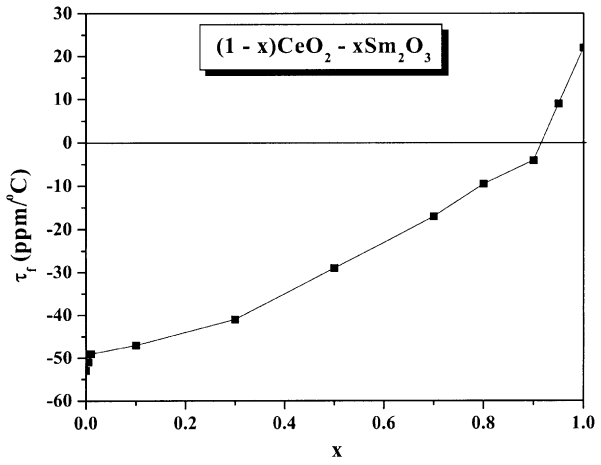

Fig. 13. Temperature coefficient of resonant frequency (τ_f) of $(1-x)CeO_2$–Sm_2O_3 ceramics as a function of composition x.

4. Conclusions

The $(1-x)$ CeO_2–$xCaTiO_3$ $(0.1 \leqslant x \leqslant 0)$ and $(1-x)CeO_2$–Sm_2O_3 $(0 \leqslant x \leqslant 1)$ dielectric ceramics have been prepared by conventional solid state ceramic route. X-ray diffraction, SEM and Raman studies indicate that CeO_2–$CaTiO_3$ form a solid solution phase. The ε_r increases, Q decreases and τ_f increases with $CaTiO_3$ addition. The ε_r of ceria increases with the addition of $CaTiO_3$, but decreases with Sm_2O_3 addition. Complete temperature stability is achieved by the addition of 5.7 mol% of $CaTiO_3$ to CeO_2. In the case of $(1-x)CeO_2$–xSm_2O_3 the Q increases up to about $x=0.5$ beyond which the Q decreases and temperature compensation occurs at $x=0.92$. The microwave dielectric properties

Table 1
Microwave dielectric properties of 1 mol% rare earth (RE) doped ceria

RE	$Q \times f$ (GHz)	ε_r	τ_f (ppm/K)
Nd	51,000	22.80	−63
Sm	90,000	23.93	−50
Eu	30,000	24.00	−78
Gd	48,000	24.20	−55
Er	74,000	23.50	−60

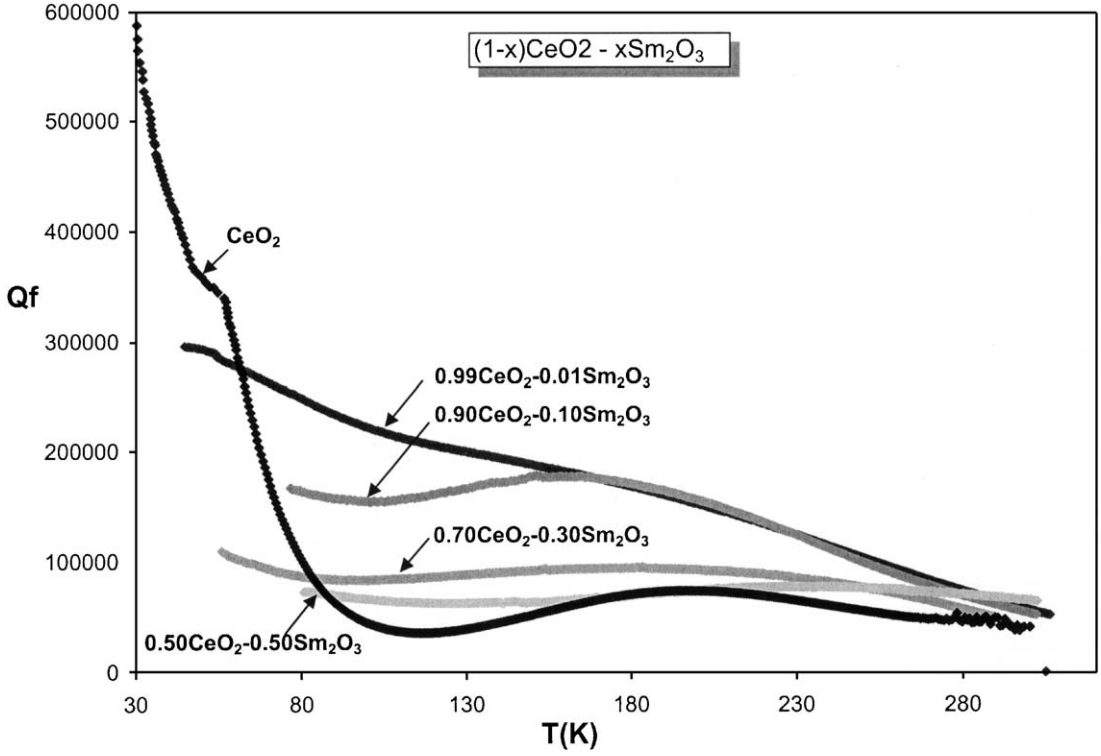

Fig. 14. Variation of quality factor ($Q \times f$ GHz) as a function of temperature on cooling.

of ceria are not depended on the ionic radius of the dopant rare earth ions. SEM studies show that addition of Sm_2O_3 and $CaTiO_3$ reduces the grain size of the CeO_2 ceramics.

Acknowledgements

The authors are grateful to DST, Government of India, New Delhi and Engineering and Physical Sciences Research Council, UK for financial assistance. One of the authors (MTS) gratefully acknowledges the EPSRC for the award of a visiting scientist position.

References

1. Wersing, W., Microwave ceramics for resonators and filters. *Current Opinion in Solid State Materials*, 1996, **1**, 715–731.
2. Dikmen, S., Shuk, P. and Greenblatt, M., Hydrothermal synthesis and properties of $Ce_{1-x}La_xO_{2-d}$ solid solutions. *Solid State Ionics*, 1999, **126**, 89–95.
3. Santha, N, Sebastian, M. T., Mohanan, P., Alford, N., Mc Neil, Puller, R. C., Sarma, V. K., Kamba, S., Pashkin, A., Samukhina, P. and Petzelt, J., Effect of doping on the dielectric properties of CeO_2 in the microwave and submillimeter frequency range. *J. Amer. Ceram. Soc.* (in press).
4. Santha, N., Jawahar, I. N., Mohanan, P. and Sebastian, M. T., Microwave dielectric properties of $(1-x)CaTiO_3$–$xSm(Mg_{1/2}Ti_{1/2})O_3$ ceramics. *Mater. Lett.*, 2002, **54**, 318–322.
5. Sreemoolanadhan, H., Issac, J., Sebastian, M. T., Jose, K. A. and Mohanan, P., Synthesis characterization and properties of $Ba_{1-x}Sr_x(Nd_{0.5}Nb_{0.5})O_3$ ceramics for application as dielectric resonator in microwave circuits. *Ceramics International*, 1995, **21**, 385–389.
6. Huang, C. L., Yang, R. Y. and Weng, M. H., Dielectric properties of $CaTiO_3$–$Ca(Mg_{1/3}Nb_{2/3})O_3$ ceramic system at microwave frequency. *Jpn. J. Appl. Phys.*, 2000, **39**, 6608–6611.
7. Ohsato, H., Atsushi, A., Takagi, Y. T., Nishigaki, S. and Okuda, T., Microwave dielectric properties and sintering of $Ba_{6-3x}R_{8+2x}Ti_{18}O_{54}$($R$ = Sm, $x = 2/3$) solid solution with added rutile. *Jpn. J. Appl. Phys.*, 1998, **37**, 5357–5359.
8. Kim, D. H., Lim, S. K. and An, C., The microwave dielectric properties of $xTiO_2$–$(1-x)CeO_2$ ceramics. *Mater. Lett.*, 2002, **52**, 240–243.
9. Wise, P. L., Reaney, I. M., Lee, W. E., Price, T. J., Iddles, D. M. and Cannel, D. S., Structure-microwave property relationship in $(Sr_xCa_{1-x})_{n+1}Ti_{n+n}O3_{n+1}$. *J. Eur. Cer. Soc.*, 2001, **21**, 1723–1726.
10. Hakki, B. W. and Coleman, P. D., Dielectric resonator method of measuring inductive capacities in the millimeter range. *IEEE Trans. Microwave. Theory. Technol.*, 1970, **MTT-8**, 402–410.
11. Courtney, W. B., Analysis and evaluation of a method of measuring the complex permittivity and permeability of microwave insulators. *IEEE Trans. Microw. Theory Technol. 1970, MTT-18*, 1970, 476–485.
12. Krupka, J., Derzakowski, K., Riddle, B. and Jarvis, J. B., A dielectric resonator for measurements of complex permittivity of low loss dielectric materials as a function of temperature. *Meas. Sci. Technol.*, 1998, **9**, 1751–1756.
13. Kim, D. H., Lim, S. K., An, C. and Kim, J. C., Microwave Dielectric Properties of $xMgTiO_3$–$(1-x)(Na_{1/2}Lni_{12})TiO_3$ Ceramics. *J. Mater. Sci.: Mater. Electron.*, 1999, **10**, 673–676.
14. Peng, C., Wang, Y., Jiang, K., Bin, B. Q., Liang, H. W., Feng, W. J. and Meng, J., Study on the structure change and oxygen vacation shift for $Ce_{1-x}Sm_xO_{2-y}$ solid solution. *J. Alloys and Compounds*, 2003, **349**, 273–278.